

ASSESSMENT OF CHEMICAL MODIFICATIONS ON THE PHOTOPHYSICAL  
PROPERTIES AND STABILITY OF ISOINDOLE MOIETIES

by

Christopher Michael Larson

HONORS THESIS

Submitted to Texas State University  
in Partial Fulfillment  
of the Requirements for  
Graduation in the Honors College

San Marcos, Texas  
May 2020

Thesis Supervisor:

Shane R. Yost

**COPYRIGHT**

by

Christopher Michael Larson

2020

## **FAIR USE AND AUTHOR'S PERMISSION STATEMENT**

### **Fair Use**

This work is protected by the Copyright Laws of the United States (Public Law 94-553, section 107). Consistent with fair use as defined in the Copyright Laws, brief quotations from this material are allowed with proper acknowledgement. Use of this material for financial gain without the author's express written permission is not allowed.

### **Duplication Permission**

As the copyright holder of this work I, Christopher Michael Larson, authorize duplication of this work, in whole or in part, for educational or scholarly purposes only.

## **Dedication**

I would like to say a big ‘thank you’ to my fellow childhood best friends and chemistry family I have made over the years, for their continued supportive reassurance. Finishing this degree was not easy, but I couldn’t have seen myself where I am now without each and every one of them.

I would like to also thank my mom and dad for their never-ending love and support throughout my undergraduate career. I fought tooth and nail in order to achieve what I have done thus far, and though they don’t live right down the road, they were nothing but a phone call away. This degree is for them. I love you both.

I will take the experience and knowledge I’ve gained from my two degrees with me into the next chapter of my life; as I continue my education and research in veterinary school.

Eat ‘Em Up Cats and thank you for everything.

—

## **Acknowledgements**

I would like to thank my supervisor, professor and mentor Dr. Shane Yost for his patience and continued response to all of my questions, as I battled through the ins and outs of computational research. He has made the world of computation much more interesting and worth all of the late nights, video meetings, hard work, and headaches from energy drinks.

I would also like to thank my lab mates from Dr. Yost's research group that aided in answering any questions I had during my time conducting research. Thank you for putting up with my obnoxious music and loud singing when I would not bring my headphones.

—

## Table of Contents

<b>DEDICATION</b> .....	<b>IV</b>
<b>ACKNOWLEDGEMENTS</b> .....	<b>V</b>
<b>TABLE OF CONTENTS</b> .....	<b>VI</b>
<b>ABSTRACT</b> .....	<b>VII</b>
<b>BACKGROUND</b> .....	<b>1</b>
<i>COMPUTATIONAL CHEMISTRY</i> .....	1
<i>DFT AND TDDFT</i> .....	1
<i>ISOINDOLES AND MEDICINAL IMPLICATIONS</i> .....	2
<i>Figure 1. Isoindole skeleton Lewis structure.</i> .....	2
<i>OVERVIEW</i> .....	3
<b>METHODS</b> .....	<b>5</b>
<i>Figure 2. Isoindole moieties of Molecule 1, created during experimentation.</i> .....	5
<i>FINDING OPTIMAL GEOMETRY—GROUND STATE ENERGY</i> .....	6
<i>Figure 3. Molecule 1's initially generated input geometry (left) and output optimized geometry (right).</i> .....	7
<i>FINDING EXCITED STATES—EMISSION AND ABSORBANCE</i> .....	7
<i>ATTACHMENT AND DETACHMENT PLOTS</i> .....	9
<i>Figure 4. Attachment (left) and detachment (right) plots rendered on moiety: Molecule 1.</i> .....	10
<i>HYDROGEN RESONANCE</i> .....	10
<i>Figure 5. Resonance structure between the R<sup>3</sup> carbon and its corresponding hydrogen and the nitrogen within the 5-member ring.</i> .....	10
<b>RESULTS</b> .....	<b>12</b>
<i>Table 1. The absorbance energy and emission energy in electron volts as well as the Stokes shift for each moiety.</i> .....	12
<i>Table 2. The carbon-hydrogen distance in angstroms for the R<sup>3</sup> carbon-hydrogen bond and the Mulliken partial charge on that carbon in atomic units for each moiety.</i> .....	12
<i>Figure 6. Attachment (green) and detachment (blue) plots for molecules 1,4,9 and 11.</i> .....	13
<i>Figure 7. Attachment and detachment plot for Molecule 11 in the ground state.</i> .....	14
<i>Table 3. The energy difference between the 1H-Isoindole and 2H-Isoindole in kcal/mol.</i> .....	14
<b>DISCUSSION</b> .....	<b>16</b>
<i>STOKES SHIFT</i> .....	16
<i>CARBON-HYDROGEN DISTANCE AND MULLIKEN ENERGY</i> .....	16
<i>ATTACHMENT AND DETACHMENT PLOTS</i> .....	17
<i>HYDROGEN RESONANCE</i> .....	18
<b>CONCLUSIONS</b> .....	<b>19</b>
<b>APPENDIX</b> .....	<b>20</b>
<b>REFERENCES</b> .....	<b>21</b>
<b>VITA</b> .....	<b>22</b>

## Abstract

Isoindoles are used in biochemical and biomedical applications for drug delivery as medication releasing agents. However, they are not stable in biological conditions. Different isoindole derivatives were theoretically created typically with structural changes via addition of functional groups to the stationary isoindole structure. These derivatives were analyzed via computational software using the time-independent, linear response form of Time Dependent Density Functional Theory (TDDFT). The absorption and emission energies were characterized for each molecule, as well as bond distances, partial charges and valence electron states. Small chemical modifications were found to produce significant changes in the properties of these molecules, some of which show increased stability. Of the 11 moieties, molecules 9 and 11 show significant deviations in the Stokes shift from the skeleton molecule, molecule 1. No real correlation was found between the  $R^3$  side group carbon-hydrogen distance and the Mulliken partial charge on the carbon. Attachment and detachment plots displayed molecule 11 is in a charge-transfer state and not favored. Molecules 1, 4 and 9 attachment and detachment plots exhibit a valence-excited state. Molecules 4, 5, 8, and 10 had energy differences between the 1H-Isoindole and 2H-Isoindole that resemble increased stability, where molecules 7 and 9 displayed lower energy differences and lower stability.

## Background

### *Computational Chemistry*

Computational chemistry is the branch of chemistry that uses the results of theoretical chemistry to solve chemistry related problems. It also involves advanced mathematical theory, which deals with the performing of simulations using fundamental equations that are derived from the Schrödinger equations.<sup>1</sup> It is well known that computational simulations can play an important role in understanding relationships between structural and optical properties in molecules.<sup>2</sup>

Computational chemistry is widely used in industries such as pharmaceutical to explore interactions of potential drugs, as well as materials science to investigate properties of plastics or industry labs to study catalysis in important reactions.<sup>3</sup> It can be used to investigate matters of: molecular geometry; chemical reactivity; IR, UV and NMR spectra; interactions between substrates and enzymes; and physical properties of substances.

### *DFT and TDDFT*

Density Functional Theory (DFT) is the most widely used computational method that often provides the best compromise between computational accuracy and cost. A functional is a mathematical entity related to a function, described as a function of a function. This is similar to a derivative of a function based off of another function.<sup>4</sup> Within DFT, the choice of functional that acts on the density determines the accuracy of the method. DFT calculations are based on the Schrödinger equation, but uses the electron density directly, bypassing the need for multielectron wavefunctions.<sup>3,4</sup> Electron density is the probability of finding any one electron within the complex somewhere in space,

whereas the wavefunction depends on all electrons within the complex. The use of the electron density instead of the full wavefunction greatly simplifies the problem and makes it possible to run on large molecules and complexes.

Time-dependent density functional theory (TDDFT)<sup>5</sup> has become one of the most popular quantum chemical approaches for calculating electronic spectra of medium-sized and large molecules.<sup>6</sup> Most TDDFT calculations are actually using the time-independent, linear response form of TDDFT. This is what was used during this research. For accurate predictions of the excited states within TDDFT, one must use what are known as range-separated functionals. If this is not done TDDFT can yield qualitatively inaccurate results.<sup>6</sup>

#### *Isoindoles and Medicinal Implications*

Isoindoles in general are reactive and unstable and they eluded isolation until the 1950's.<sup>7</sup> In spite of their 10- $\pi$ -electron aromatic structure, N-substitution, aryl, and halogen substitution are usually required to increase the stability of isoindoles that are not conjugated with other unsaturated functional groups.<sup>7</sup>

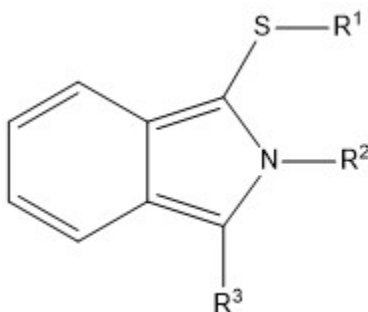


Figure 1. Isoindole skeleton Lewis structure.<sup>7</sup>

They are used in biochemical and biomedical applications such as drug delivery of medication as a releasing agent, fluorescent tagging of amino acids in studying the

mechanism of action within viral or bacterial infected cells, and implementation within polymerase-1 inhibitors in cancer therapies such as radiation and chemotherapy.<sup>8-10</sup>

*Figure 1* displays the Lewis structure of the thiol isoindole skeleton molecule without the addition of side-groups R<sup>1</sup>-R<sup>3</sup>. For the purpose of this research, side-groups R<sup>1</sup> and R<sup>2</sup> will all contain the same alkyl side chains (R<sup>1</sup>: ethane, R<sup>2</sup>: butane). The side-group position R<sup>3</sup> is the most unstable. All molecules with the exception of one moiety did not add any side-groups to the R<sup>3</sup> position.

### *Overview*

The research conducted was done for means of pharmaceutical application and the parameters explored were molecular modifications and their impact on the photophysical properties of the isoindole moieties. Isoindoles are very unstable, and in order to use them for drug delivery implications, the complex needs to be more manageable. This research takes a base thiol isoindole (*Figure 1*) and creates 10 additional moieties in order to compare their stability and photophysical properties: absorbance energy, emission energy, Stokes shift, bond strength, transition states, and Mulliken energy for the excited states in order to find the more stable molecule complex. The isoindole moieties used were suggested by Dr. Kornienko, an organic chemist at Texas State University, and his research lab based on what molecules could be reasonably synthesized. All of the molecules were designed to withdraw electron density from the five-member ring in the isoindole complex in hopes of increasing the stability at the R<sup>3</sup> position.

I hypothesize, the addition of electron withdrawing groups will stabilize the molecules while leaving the excited states photophysical properties unchanged. The presence of electron withdrawing groups increase the overall electronegativity of the molecule, by

pulling the electron density from available electrons within the structure and induces the density and spreads it out. Doing this stabilizes the molecule. The lowest lying excitation in the isoindole molecule is a  $\pi \rightarrow \pi^*$  transition. For the modifications that do not modify the  $\pi$  conjugated orbitals we expect the excited state properties to remain relatively unchanged.

## Methods

A total of 11 isoindole moieties (**Figure 2**) were generated using the computational software QChem. QChem is a software system that brings together a variety of advanced computational methods and tools, greatly improving the speed and accuracy of calculations being performed. Molecule 1 was the reference molecule and molecules 2-11 consisted of the additions of functional groups, cyclic rings and halides. The text editing software Kate was utilized to modify input files and open and read output files. Each molecule's initial geometry was generated using the IQmol extension of QChem. The geometries were optimized within QChem using the  $\omega$ B97x-V functional and the cc-pvtz basis set.

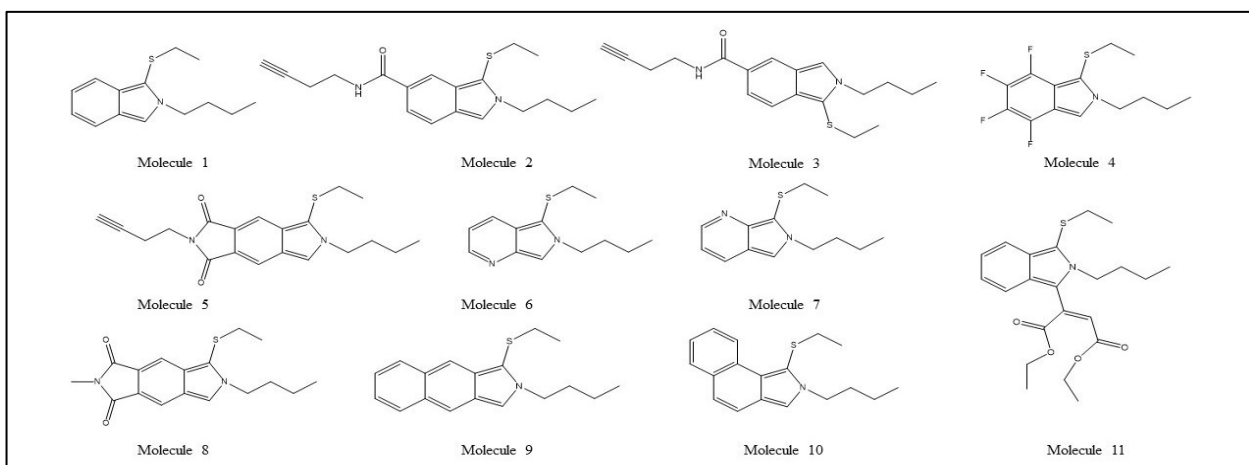


Figure 2. Isoindole moieties of Molecule 1, created during experimentation.

The excited state energies, absorption and emission, for the 11 moieties were found utilizing the TDDFT method in the QChem software with alternative parameters for each calculation being set in each input file. Following the excited state calculations, attachment and detachment plots were ran in QChem under a new parameter set and viewed in IQmol. IQmol was utilized within the QChem software as a free-form molecule builder and comprehensive interface for setting up the input for the QChem jobs.

### *Finding Optimal Geometry—Ground State Energy*

Each molecule was first created via a ball-and-stick format on IQmol. This was the first part of finding the optimal geometry. Each molecule was estimated in regard to placement of each bond and molecule. The created structure was then minimized within IQmol, by placing molecules in the ideal geometry based on the estimated placement of the created structure. This included bond angle rearrangements and bond length adjustments. IQmol generated XYZ coordinates for each elemental atom. These coordinates are saved under IQmol as an .xyz file onto the QChem software. The '.xyz' file was then opened using Kate. The following parameters were set in order to run the DFT optimal geometry calculation:

```
$molecule
0 1
...
$end

$rem
BASIS = cc-pVTZ
GEOM_OPT_MAX_CYCLES = 200
GUI = 2
INCDFT = 0
INCFOCK = 0
JOB_TYPE = Optimization
METHOD = wB97XV
SCF_CONVERGENCE = 8
SCF_MAX_CYCLES = 200
SYMMETRY_IGNORE = 1
SYMMETRY_INTEGRAL = 0
SYMMETRY = 0
$end
```

Each molecule's coordinates were saved into an appropriately labeled input file, '.inp' containing the parameters to run the calculation. Each molecule's calculation ran until converged using equation (A1).

After the geometry optimization calculation was complete, each input file generated a corresponding output file '.out' and '.out.fchk' file, which when opened in IQmol, generated the optimized ball and stick model of the molecule, as seen in **Figure 3**.

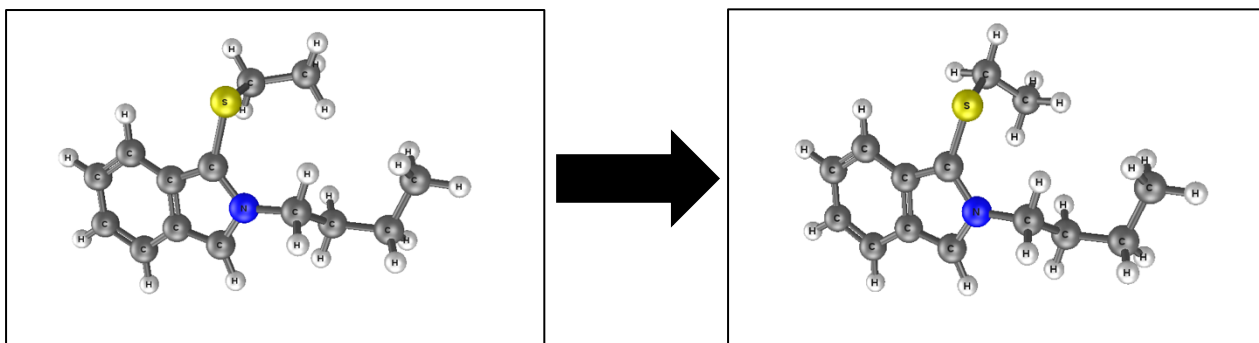


Figure 3. Molecule 1's initially generated input geometry (left) and output optimized geometry (right).

The XYZ coordinate values for each element in the molecule were taken from the now optimized output file, renamed according to each molecule's designated label (ex. *Molecule 1*) and stored in QChem for further analysis. This geometry was utilized for finding the emission and absorbance energy.

#### *Finding Excited States—Emission and Absorbance*

The converged XYZ coordinate values were copied from the ground state optimization and pasted into a fresh Kate file, '.tddft.inp' for each molecule respectively. The absorption energy was calculated using a TDDFT calculation with the parameters:

```
$molecule  
0 1  
...  
$end
```

```

$rem
  BASIS = cc-pVTZ
  METHOD = wb97XV
  CIS_N_ROOTS = 8
  CIS_SINGLETS = TRUE
  CIS_TRIPLETS = TRUE
  RPA = TRUE
  SYMMETRY = FALSE
  SYM_IGNORE = TRUE
  INCFOCK = FALSE
  INCDFT = FALSE
  GUI = 2
$end

```

Utilizing equation (*AI*), the lowest singlet absorption energies were obtained through the output files and tabulated respectively.

Using the same geometry used in the absorption energy calculations, a new file was created for each moiety. The files, '.qchem.tddft.opt.inp' utilized equation (*AI*) in order to obtain the minimum geometry for the lowest energy singlet excited state using a TDDFT calculation with the following parameters:

```

$molecule
0 1
...
$end

$rem
  BASIS = 6-31G*
  METHOD = wb97x-D
  CIS_N_ROOTS = 8
  CIS_SINGLETS = TRUE
  CIS_TRIPLETS = FALSE
  RPA = TRUE
  SYMMETRY = FALSE
  SYM_IGNORE = TRUE
  INCFOCK = FALSE
  INCDFT = FALSE
  GUI = 2
  CIS_STATE_DERIV = 1
  JOBTYP = OPT
$end

```

The final emission state geometry was copied from the '.qchem.tddft.opt.out' file and pasted into a new Kate file. The new file for each moiety contained the parameters used in the absorption energy '.tddft.inp' calculation and was re-run. This calculation used a larger basis set to obtain more accurate results. The lowest singlet emission energy was collected and tabulated from the output file.

#### *Attachment and Detachment Plots*

Using the optimal ground state geometry from the absorption '.tddft.inp' file, the parameters were used to generate attachment and detachment plots for moieties 1, 4, 9, 11:

```
$molecule
0 1
...
$end

$rem
  BASIS = cc-pVTZ
  METHOD = wB97XV
  CIS_N_ROOTS = 8
  CIS_SINGLETs = TRUE
  CIS_TRIPLETs = TRUE
  RPA = TRUE
  SYMMETRY = FALSE
  SYM_IGNORE = TRUE
  INCFOCK = FALSE
  INCDFt = FALSE
  GUI = 2
  PLOTS = TRUE
  MAKE_CUBE_FILES = TRUE
$end

$plots
  ATTACHMENT_DETACHMENT_DENSITY = 1
$end
```

Calculations ran for moieties 1, 4, 9, 11 using equation (A2) to generate the molecular orbital files and the files containing the plots.

The plots were accessible by opening the 'molecule.mos' file → opening the 'plots' file → then opening the 'attach\_a.1 cube' and 'detach\_a.1 cube' files through IQmol. In IQmol, each file was double clicked to open additional settings. The isosurface value was lowered to 0.002, the attachment color was set to green, and the detachment color was set to blue (Figure 4).

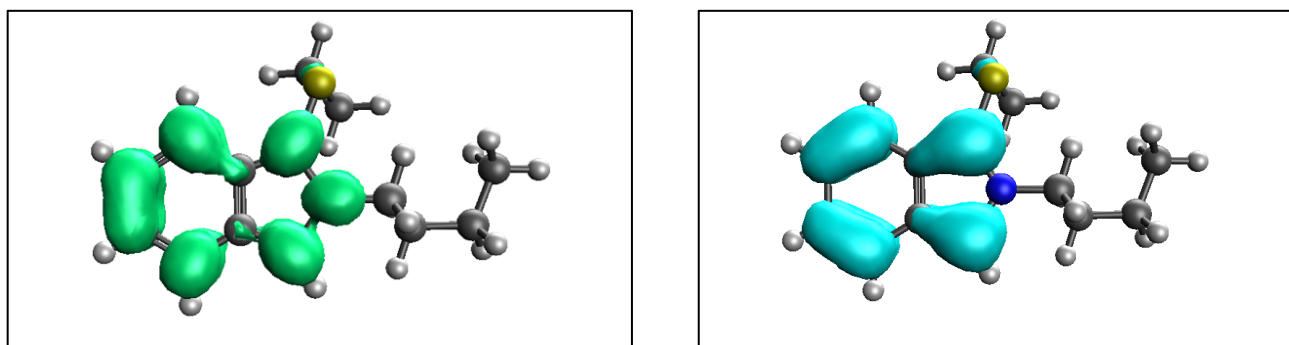


Figure 4. Attachment (left) and detachment (right) plots rendered on moiety: Molecule 1.

### Hydrogen Resonance

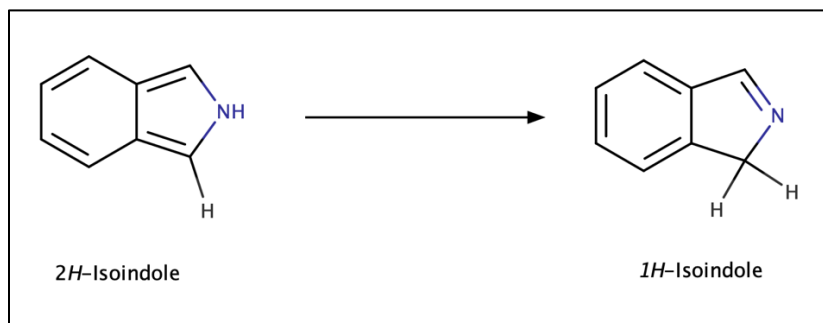


Figure 5. Resonance structure between the R<sup>3</sup> carbon and its corresponding hydrogen and the nitrogen within the 5-member ring.

Using the optimal ground state geometry, the moieties 1-10 were opened in IQmol and a hydrogen from the R<sup>3</sup> carbon position was placed onto the nitrogen (Figure 5) within the

5-member cyclic ring. The geometry was optimized for each moiety, the same way the ground state geometry was optimized utilizing the parameters:

```
$molecule
0 1
...
$end

$rem
BASIS = cc-pVTZ
GEOM_OPT_MAX_CYCLES = 200
GUI = 2
INCDFT = 0
INCFOCK = 0
JOB_TYPE = Optimization
METHOD = wB97XV
SCF_CONVERGENCE = 8
SCF_MAX_CYCLES = 200
SYMMETRY_IGNORE = 1
SYMMETRY_INTEGRAL = 0
SYMMETRY = 0
$end
```

The final energies were recovered by taking the difference between the two ground state energies and were tabulated accordingly.

## Results

Molecule	Abs $eV$	Emis $eV$	Stokes Shift
1	4.2391	3.2193	1.0198
2	4.0430	3.1326	0.9104
3	4.1331	3.2758	0.8573
4	4.3538	3.2436	1.1102
5	4.0090	3.1646	0.8444
6	4.1275	3.0489	1.0786
7	3.9438	2.903	1.0408
8	4.0279	3.1124	0.9155
9	3.2610	2.7448	0.5162
10	4.4529	3.6034	0.8495
11	3.7434	2.0855	1.6579

Table 1. The absorbance energy and emission energy in electron volts as well as the Stokes shift for each moiety.

The absorption and emission energy ( $eV$ ; electron volts) were collected and tabulated (**Table 1**) along with the Stokes shift for each of the 11 moieties. The green color for each column displays the highest value and the red displays the lowest value for each column respectively.

Molecule	C-H Distance ( $\text{\AA}$ )	Mulliken ( <i>a. u.</i> )
1	1.07960	-0.265090
2	1.07981	-0.279435
3	1.08001	-0.277902
4	1.07850	-0.262621
5	1.07995	-0.258095
6	1.07867	-0.223325
7	1.07964	-0.277603
8	1.07997	-0.259950
9	1.07975	-0.287287
10	1.08028	-0.269556
11	-----	-----

Table 2. The carbon-hydrogen distance in angstroms for the  $R^3$  carbon-hydrogen bond and the Mulliken partial charge on that carbon in atomic units for each moiety.

The distance between the R<sup>3</sup> carbon and its corresponding hydrogen were tabulated (**Table 2**) in angstroms ( $\text{\AA}$ ) along with the Mulliken charge on the carbon in atomic units (*a. u.*) for each moiety. The green color for the carbon-hydrogen distance column displays the farthest distance of the hydrogen from the carbon and the red showing the closest. The green color for the Mulliken energy represents the most negative value and the red being the least negative value. Molecule 11 was not included since its chemical modification involved replacing the R<sup>3</sup> carbon-carbon bond with a carbon-hydrogen bond.

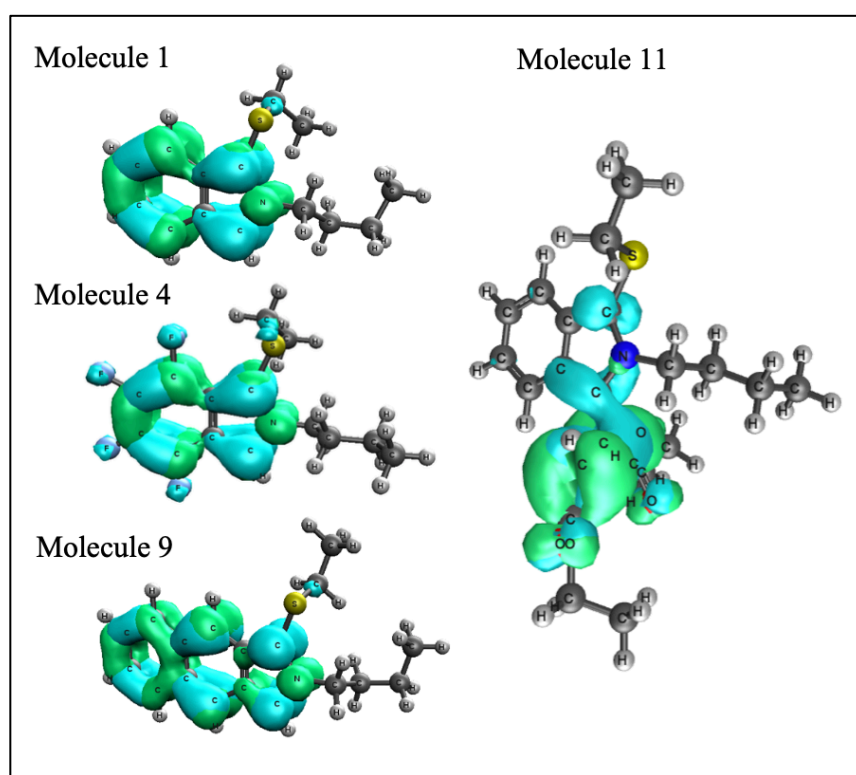


Figure 6. Attachment (green) and detachment (blue) plots for molecules 1, 4, 9 and 11.

**Figure 6** depicts attachment and detachment plots for molecules 1, 4, 9 and 11. The green represents the attachment, which is where the electron went to. Whereas the blue represents the detachment, which is where the electron came from. Elemental legend: dark gray represents carbon; light gray represents hydrogen; yellow represents sulfur; dark blue

represents nitrogen; red represents oxygen. These plots are used to analyze the type of excited state present.

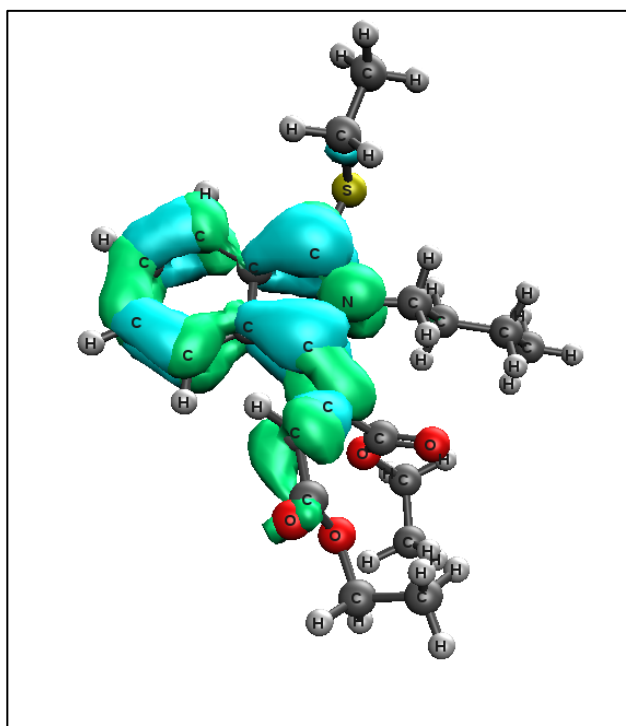


Figure 7. Attachment and detachment plot for Molecule 11 in the ground state.

An attachment and detachment plot was taken for Molecule 11 in the molecules ground state and display a partial valence-excited state (**Figure 7**).

Molecule	$\Delta E$ kcal/mol
1	1.699
2	2.494
3	2.873
4	3.340
5	5.754
6	2.241
7	0.138
8	5.275
9	-5.115
10	8.114

Table 3. The energy difference between the 1H-Isindole and 2H-Isindole in kcal/mol.

**Table 3** depicts the energy difference calculated between the ground state energies of the 1H-Isoindole and 2H-Isoindole (**Figure 5**). The column on the right of the table indicates the change in energy (kcal/mol) of reaction between the resonance of moving a hydrogen molecule from the nitrogen atom within the 5-member isoindole complexes and the R<sup>3</sup> carbon. The green indicates the larger and more positive values and the red indicates the smaller and more negative values.

## Discussion

The data collected displays the results of calculations being used to draw assumptions about the eleven moieties.

### *Stokes Shift*

Of the eleven molecules, the lowest singlet energy was recovered for both the absorbance and emission energies (**Table 1**). The Stokes shift displays the difference between the two energies. Molecules with a lower valued Stokes shift are said to be more ridged and stiffer due to the addition and location of side-groups that were added to the isoindole skeleton (**Figure 1**). This can be seen in molecules 9 and 10, displaying lower Stokes shift values due to the addition of C-C bonds to create an additional cyclic ring. These values compared to molecules 6 and 7, which have a higher Stokes shift with the addition of a nitrogen atom into the 6-membered cyclic ring, are more ridged in structure and assumed to be more stable. Out of all of the suggested changes to stabilize the isoindole complex, it is only molecules 9 and 11 that show significant deviations from the original absorption/emission of the isoindole skeleton, Molecule 1. The excited state properties of isoindole are ideal for their applications, hence we don't want them to change while stabilizing the molecule.

### *Carbon-Hydrogen Distance and Mulliken Energy*

Relatively speaking the distance/bond length between the R<sup>3</sup> carbon and its hydrogen can be calculated and used to assist in determining the stability and bond strength within the molecule. The R<sup>3</sup> carbon within the isoindole gives off a carbon partial charge, known as the Mulliken charge (*a. u.*). These two values show possible correlation (**Table 2**), as

the carbon-hydrogen bond distance is shorter, that carbon should be less negatively charged. Shorter bonds are similar to a higher bond order.

These two parameters were chosen initially to study the stability of the isoindole moieties, since they are very simple to compute and would be ideal if they could be used to screen stability. In chemistry, we know a triple bond within two molecules is stronger than a double or single bond. A triple bond is also shorter in length between the two molecules compared to a double and single bond. Respectively, a carbon-hydrogen bond distance that is shorter in length should be stronger and supply more structure and stability to the molecule, compared to a longer distance.

The R<sup>3</sup> carbon within the 5-member cyclic ring has a partial charge on it. This partial charge is predicted to be correlated with the bond distance between the hydrogen. If the partial charge on the carbon is more negative, the bonded hydrogen is not going to want to fill carbons valence shell as strongly as it would to a carbon with a less negative partial charge. In theory, if the Mulliken charge is less negative, the carbon-hydrogen bond should be shorter, and the bond would then be stronger. Thus, resulting in a more stable molecule. What is found is not a real correlation between the two values: a shorter distance will yield a less negative partial charge. Therefore, a more detailed study was performed on the hydrogen resonance, depicted in *Figure 5*, since it is believed that the 1H-Isoindole is a more reactive species in solution.

#### *Attachment and Detachment Plots*

In molecule 11 (*Figure 6*) it is noted that it is a charge-transfer state while in its excited state. This is noted by the movement of the valence electrons from where they attach and detach. If the attachment and detachment colors are spread out along the side groups and

no longer within the isoindole bi-cyclic structure it is deemed a charge-transfer state. A charge-transfer state is not desirable as it has low to no absorbance and emission, thus Molecule 11 won't fluoresce. This is noted in **Figure 7**, where molecule 11 exhibits what is suspected to be a valence-excited state but moved to a charge-transfer in the molecules excited state. This is supported by the very large Stokes shift for Molecule 11 (**Table 1**) as well as the computed emission intensity is significantly lower than the absorption. Molecules 1, 4 and 9 (**Figure 6**) are in a valence-excited state by maintaining the exchange of the valence-electrons within the bi-cyclic structure. Their absorption and emission intensities did not significantly change,  $\cong 15\%$ , between the absorption and emission states.

#### *Hydrogen Resonance*

The energy difference between the 1H-Isoindole and 2H-Isoindole was recovered and the resonance of the hydrogen atom was studied. It is believed that the 1H-Isoindole is more reactive than the 2H-Isoindole configuration. There is potential to believe that the more stable the 2H-Isoindole configuration is, the more stable the molecule will be. In Table 3, molecules 4, 5, 8, and 10 should be more stable in solution, while molecules 7 and 9 are predicted to be even less stable. A positive value represents the 1H-Isoindole structure is higher in energy than the 2H-Isoindole.

## Conclusions

In my thesis, I hypothesized that the emission and absorption energies could be maintained while stabilizing the isoindole molecules through the addition of electron withdrawing groups. I used the QChem software to compute the optimal geometry for each moiety and utilized the optimal geometry to find the Stokes shift between the emission and absorbance energies as well as formulating attachment and detachment plots. New optimal geometries were found for each moiety from the 1H-Isoindole and 2H-Isoindole structures.

I found through analyzing the Stokes shift for the 11 moieties that molecule 9 and molecule 11 displayed significant deviations from the absorbance and emission of the original isoindole molecule, Molecule 1. Analyzing the possible correlation between the carbon-hydrogen distance of the R<sup>3</sup> side group carbon and the Mulliken partial charge on the R<sup>3</sup> carbon, resulted in no real significance in correlation between the two factors. In the attachment and detachment plots it was concluded that molecules 1, 4 and 9 were in a valence-excited state which is favored for the purpose of this research over molecule 11 which displayed a charge-transfer excited state. The energy difference for moieties 1-10, between the 1H-Isoindole and 2H-Isoindole structures, yields molecules 4, 5, 8 and 10 are more stable in solution with a higher change in energy, compared to molecules 7 and 9 which are predicted to be less stable due to the smaller difference in energy.

Based on the data collected, I conclude that the additions of electron withdrawing groups in molecules 4, 5, 8, 10 are presenting to be the more stable molecules out of the 11 moieties, and the addition of the electron withdrawing groups in molecules 7, 9, and 11 are presenting to be the lesser stable molecules

## Appendix

*Finding Optimal Geometry (p. 6)*

*sqthis -t openmp --ppn=14 --parallel=14 filename.inp* (A1).

*Finding Excited States (p. 7)*

*sqthis -t openmp --ppn=14 --parallel=14 -savefiles filename.inp* (A2).

## References

- (1) Janjua, M. R. S. A. Structural Properties and Nonlinear Optical Responses of Halogenated Compounds: A DFT Investigation on Molecular Modelling. *Open Chem.* **2018**, *16* (1), 978–985. <https://doi.org/10.1515/chem-2018-0113>.
- (2) Amat, A.; Miliani, C.; Romani, A.; Fantacci, S. DFT/TDDFT Investigation on the UV-Vis Absorption and Fluorescence Properties of Alizarin Dye. *Phys. Chem. Chem. Phys.* **2015**, *17* (9), 6374–6382. <https://doi.org/10.1039/C4CP04728A>.
- (3) Lewars, E. G. *Computational Chemistry*; Springer International Publishing: Cham, 2016. <https://doi.org/10.1007/978-3-319-30916-3>.
- (4) Bondoc, J. For Graduation in the Honors College. 21.
- (5) Recent Advances In Density Functional Methods, Part I  
<http://web.b.ebscohost.com.libproxy.txstate.edu/ehost/ebookviewer/ebook/ZTAWMHhuYV9fNTY0NDcxX19BTg2?sid=db8d34c1-4b6d-4f7c-bdea-a405a4e6beb2@sessionmgr101&vid=0&format=EB&rid=1> (accessed Mar 4, 2020).
- (6) Dreuw, A.; Head-Gordon, M. Failure of Time-Dependent Density Functional Theory for Long-Range Charge-Transfer Excited States: The Zincbacteriochlorin–Bacteriochlorin and Bacteriochlorophyll–Spheroidene Complexes. *J. Am. Chem. Soc.* **2004**, *126* (12), 4007–4016. <https://doi.org/10.1021/ja039556n>.
- (7) Simons, S. S.; Johnson, D. F. Reaction of O-Phthalaldehyde and Thiols with Primary Amines: Formation of 1-Alkyl(and Aryl)Thio-2-Alkylisoindoles. *J. Org. Chem.* **1978**, *43* (14), 2886–2891. <https://doi.org/10.1021/jo00408a030>.
- (8) Synthesis of fluorescent ristocetin aglycon derivatives with remarkable antibacterial and antiviral activities | Elsevier Enhanced Reader  
<https://reader.elsevier.com/reader/sd/pii/S0223523412006344?token=19E0E92B874C7A2D1ECECF3861008033FBF819A424ECF2C74177725392E5D8B3F06906D0AC78A3817D039EC765C4B6F3> (accessed Mar 3, 2020).  
<https://doi.org/10.1016/j.ejmech.2012.10.030>.
- (9) Papeo, G.; Posteri, H.; Borghi, D.; Busel, A. A.; Caprera, F.; Casale, E.; Ciomei, M.; Cirila, A.; Corti, E.; D’Anello, M.; Fasolini, M.; Forte, B.; Galvani, A.; Isacchi, A.; Khvat, A.; Krasavin, M. Y.; Lupi, R.; Orsini, P.; Perego, R.; Pesenti, E.; Pezzetta, D.; Rainoldi, S.; Riccardi-Sirtori, F.; Scolaro, A.; Sola, F.; Zuccotto, F.; Felder, E. R.; Donati, D.; Montagnoli, A. Discovery of 2-[1-(4,4-Difluorocyclohexyl)Piperidin-4-Yl]-6-Fluoro-3-Oxo-2,3-Dihydro-1 H -Isoindole-4-Carboxamide (NMS-P118): A Potent, Orally Available, and Highly Selective PARP-1 Inhibitor for Cancer Therapy. *J. Med. Chem.* **2015**, *58* (17), 6875–6898. <https://doi.org/10.1021/acs.jmedchem.5b00680>.
- (10) Spanò, V.; Pennati, M.; Parrino, B.; Carbone, A.; Montalbano, A.; Cilibrasi, V.; Zuco, V.; Lopercolo, A.; Cominetti, D.; Diana, P.; Cirrincione, G.; Barraja, P.; Zaffaroni, N. Preclinical Activity of New [1,2]Oxazolo[5,4- e ]Isoindole Derivatives in Diffuse Malignant Peritoneal Mesothelioma. *J. Med. Chem.* **2016**, *59* (15), 7223–7238. <https://doi.org/10.1021/acs.jmedchem.6b00777>.

## VITA

Christopher Michael Larson was born in Baytown, Texas, on December 15<sup>th</sup>, 1997, the son of Ronald James Larson and Kimberly Ann Larson, brother of Alexander James Larson. After completing his education at Ross S. Sterling High School in 2016, he entered as a student at Lee Community College of Baytown, Texas. He moved to San Marcos in the fall of 2016 to begin his education at Texas State University. He obtained his Associates of Arts in Social Sciences in 2017 from Lee Community College. He became a research assistant to Dr. William Brittain's research lab in 2018 where he began performing synthesis under Dr. Shiva Rastogi. Christopher graduated with his Bachelor of Science in Animal Science with Pre-Veterinary emphasis and a minor in Chemistry in the summer of 2019. He later returned to Texas State University that fall, where he became a research assistant under Dr. Shane Yost performing computational research. He graduated with his Bachelor of Science in Chemistry with Pre-Medical emphasis and minors in Biology and Honors Studies in spring of 2020.

Christopher has accepted a seat for the fall semester of 2020 at Ross University School of Veterinary Medicine to begin his journey toward earning his Doctor of Veterinary Medicine (D.V.M) degree. He is currently applying for a PhD research position at Ross which he plans to be admitted and finish in 2026 along with his DVM in 2024. Christopher plans to begin a residency in either cardiovascular, emergency and critical care, or surgical medicine following the completion of his PhD. He will plan to practice for the remainder of his life until retirement, when he plans to join academia as a professor within a veterinary institution.